THE ASTROPHYSICAL JOURNAL, 525:10–16, 1999 November 1

STRUCTURE FORMATION IN THE QUASI–STEADY STATE COSMOLOGY: A TOY MODEL

ALI NAYERI, SUNU ENGINEER, AND J. V. NARLIKAR
Inter-University Centre for Astronomy and Astrophysics, Post Bag 4, Ganeshkhind, Pune 411007, India
AND
F. HOYLE
102 Admirals Walk, Bournemouth BH2 5HF Dorset, England
Received 1999 February 25; accepted 1999 June 16

ABSTRACT

The problem of formation of large-scale structure is discussed within the framework of the quasi–steady state cosmology (QSSC). The primary process of creation of matter and the resulting dynamics of ejection of matter from regions of strong gravitational fields play a key role. To understand their workings, a toy model is used, in which from a set of randomly distributed creation centers a new generation of centers is created as part of an iterative algorithm. It is shown that the system develops clusters and voids along with filamentary structure, within a few iterations. The two-point correlation function and density distribution function for these simulations are shown to reproduce the observed clustering of the large-scale structure in the real universe.

Subject headings: cosmology: theory — galaxies: clusters — galaxies: formation — large-scale structure of universe

1. INTRODUCTION

The quasi–steady state cosmology (QSSC) was first proposed in 1993 and explored further by Fred Hoyle, Geoffrey Burbidge, and Jayant Narlikar in a series of papers (Hoyle, Burbidge, & Narlikar 1993, 1994a, 1994b, 1995a, 1995b). The QSSC offers an alternative to the commonly accepted big bang cosmology, and the above work claims to provide a singularity-free cosmological model, which is consistent with the data on discrete source populations and can explain the production of light nuclei as well as the spectrum and anisotropy of the microwave background. Because the dynamical and physical conditions in this cosmology are considerably different from those in the standard cosmology, the theoretical reasoning required to understand what is observed may differ too. In short, one may not simply lift a theoretical line of reasoning from standard cosmology and expect to apply it to the same problem in the QSSC.

One of the outstanding problems in modern big bang cosmology is the problem of formation of large-scale structure in the universe. The standard approach consists in starting with prescribed primordial fluctuations of space-time geometry and matter density, evolving them through an inflationary era, having them interact with nonbaryonic dark matter, then carrying out N-body simulations of interacting masses which may eventually form into groups to be identified with large-scale structures such as galaxies, clusters, superclusters, voids, and so on. Although much of this work has gone into cosmology textbooks (see, for example, Peebles 1993 and Padmanabhan 1993), it is a fair comment to say that no unique and generally acceptable structure formation scenario has yet emerged in standard cosmology.

The problem of structure formation poses a challenge in the QSSC also, and it should be viewed against the background of the above standard approach. As we shall see in § 2, the QSSC does not have an era when the baryonic matter density in the universe was $\sim 10^{81}$ times its present value, as it was in the big bang cosmology in the immediate postinflation era. Thus the growth of fluctuations in the form of gravitational instabilities will not be similar in this cosmology to that in the big bang cosmology.

Recently the gravitational stability of the QSSC models against small perturbations was examined in detail in a paper by Banerjee & Narlikar (1997). They found the cosmological solution to be stable, and thus there was no net growth in density fluctuations. The model is basically oscillatory, and perturbations of density and metric grow only to a finite amount during the contraction phase and then decay during the expansion phase. These authors concluded that gravitational instability alone cannot lead to formation of structures in the QSSC. Instead, explosive matter creation in the so-called *minibangs* is expected to be the principal cause of forming structures. In this paper we shall make a beginning in this field and first try to understand the pattern of formation and growth of structures in the QSSC through numerical simulations by using a simplified toy model.

The organization of this paper is as follows: In § 2 we briefly review the basic theory of QSSC. The numerical toy model will be introduced in § 3. Section 4 is devoted to computing the two-point correlation function for the distributions arising in the toy model and its comparison with observations. In § 5 we conclude by highlighting the success of this approach and indicating how it can be further improved.

2. THE BASIC THEORY OF THE QSSC

The basic formulation of the QSSC is via the Machian theory of gravity first proposed by Hoyle & Narlikar (1964, 1966; see also Hoyle et al. 1995a) in which the origin of inertia is linked to a long-range scalar interaction between matter and matter. Specifically, the theory is derivable from an action principle with the simple action

$$\mathcal{A} = -\sum_a \int m_a \, ds_a \,, \tag{1}$$

where the summation is over all the particles in the universe, labeled by the index a, the mass of the ath particle

being m_a. The integral is over the worldline of the particle, ds_a representing the element of proper time of the ath particle.

The mass itself arises from interaction with other particles. Thus the mass of particle a at point A on its worldline arises from all other particles b in the universe:

$$m_a = \sum_{b \neq a} m_{(b)}(A) \,, \tag{2}$$

where $m_{(b)}(X)$ is the contribution of inertial mass from particle b to any particle situated at a general spacetime point X. The long-range effect is Machian in nature and is communicated by the scalar mass function $m_{(b)}(X)$ which satisfies the conformally invariant wave equation

$$\Box m_{(b)} + \tfrac{1}{6} R m_{(b)} + m_{(b)}^3 = N_{(b)} \,. \tag{3}$$

Here the wave operator is with respect to the general spacetime point X. R is the scalar curvature of spacetime, and the right-hand side gives the number density of particle b. The field equations are obtained by varying the action with respect to the spacetime metric g_{ik}. The important point to note is that the above formalism is conformally invariant. In particular, one can choose a conformal frame in which the particle masses are constant. If the constant mass is denoted by m_p, the field equations reduce to

$$R^{ik} - \frac{1}{2} g^{ik} R + \Lambda g^{ik} = -\frac{8\pi G}{c^4} \left[T^{ik} - f\left(C^i C^k - \frac{1}{4} g^{ik} C^l C_l \right) \right], \tag{4}$$

where c is the speed of light and C is a scalar field which arises explicitly from the ends of broken worldlines, that is, when there is creation (or annihilation) of particles in the universe. The constant f denotes the coupling of the C-field to spacetime. Thus the divergence of the matter tensor T^{ik} need not always be zero, since the creation or annihilation of particles is compensated by the nonzero divergence of the C-field tensor in equation (4). The quantities G (the gravitational constant) and Λ (the cosmological constant) are related to the large-scale distribution of particles in the universe. Thus,

$$G = \frac{3\hbar c}{4\pi m_p^2} \text{ and } \Lambda = -\frac{3}{N^2 m_p^2} \,, \tag{5}$$

N being the number of particles within the cosmic horizon.

Note that the signs of the various constants are determined by the theory and not inserted by hand. For example, the constant of gravitation is positive, the cosmological constant is negative, and the coupling of the C-field energy tensor to spacetime is negative.

2.1. *Matter Creation*

The action principle tells us that matter creation is possible at a given spacetime point provided the ambient C-field satisfies the equality $C_i C^i = m_p^2$ at that point. In normal circumstances, the background level of the C-field will be *below* this level. However, in the strong gravity obtaining in the neighborhood of compact massive objects, the value of the field can be locally raised. This leads to creation of matter along with the creation of negative C-field energy. The latter also has negative stresses which have the effect of blowing the spacetime outward (as in an inflationary model) with the result that the created matter is thrown out in an explosion. Qualitatively the creation and ejection proceeds along the following lines.

The process normally begins by the creation of the C-field along with matter in the neighborhood of a compact massive object. The former, being propagated by the wave equation, tends to travel outward with the speed of light, leaving the created mass behind. However, as the created mass grows, its gravitational redshift begins to assert itself, and the C-field gets trapped in the vicinity of the object. As its strength grows, its repulsive effect begins to manifest itself, thus making the object less and less bound and unstable. Finally, a stage may come when a part of the object is ejected from it with tremendous energy. It is thus possible for a parent compact mass to eject a bound unit outward. This unit may act as a center of creation in its own right.

We shall refer to such pockets of creation as *minibangs* or *mini–creation events* (MCEs). A spherical (Schwarzschild-type) compact matter distribution will lead to a spherically symmetric explosion, whereas an axisymmetric (Kerr-type) distribution would lead to jetlike ejection along the symmetric axis. Because of the conservation of angular momentum of a collapsing object, it is expected that the latter situation will in general be more likely.

In either case, however, the minibang is *nonsingular*. There is no state of infinite curvature and terminating worldlines, as in the standard big bang, nor is there a black hole–type horizon. The latter because the presence of the C-field causes the collapsing object to bounce outside the event horizon.

2.2. *The Cosmological Solution*

The feedback of such minibangs on the spacetime as a whole is to make it expand. In a completely steady situation, the spacetime will be that given by the de Sitter metric. However, the creation activity passes through epochs of ups and downs with the result that the spacetime also shows an oscillation about the long-term steady state. Sachs, Narlikar, & Hoyle (1996) have computed the general solutions of this kind, and the simplest such solution with the line element given by

$$ds^2 = c^2 dt^2 - S^2(t)[dr^2 + r^2(d\theta^2 + \sin^2\theta \, d\phi^2)] \,, \tag{6}$$

where c stands for the speed of light, has the scale factor given by

$$S(t) = e^{t/P}\left[1 + \eta \cos \frac{2\pi\tau(t)}{Q} \right]. \tag{7}$$

The constants P and Q are related to the constants in the field equations, while $\tau(t)$ is a function $\sim t$, which is also determined by the field equations. For details see Sachs et al. (1996). We shall, however, use the approximation $\tau(t) = t$, which is adequate for the purpose of this paper. The parameter η may be taken to be positive and is less than unity. Thus the scale factor never becomes zero: the cosmological solution is without a spacetime singularity. The form of the scale factor, $S(t)$, in the metric (eq. [6]) is shown in Figure 1.

2.3. *Observational Checks*

Hoyle et al. (1994a, 1994b) have shown that the above cosmology gives a reasonably good fit to the observations

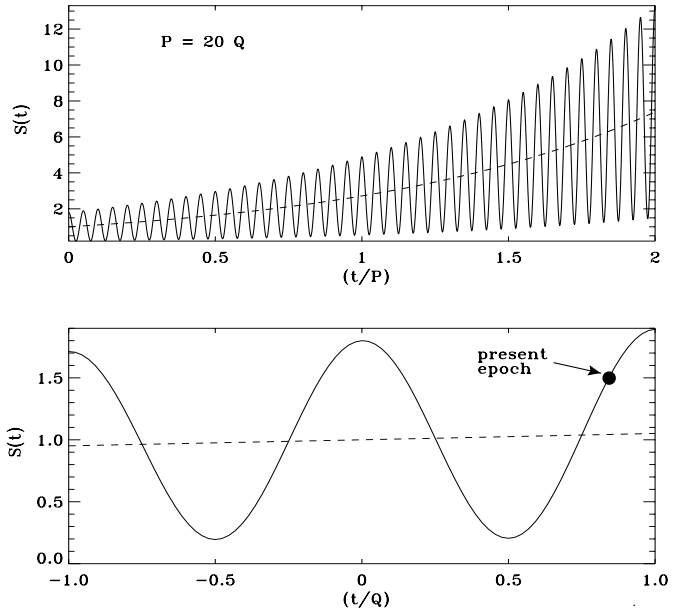

FIG. 1.—The scale factor $S(t)$ of the QSSC in the upper panel against t to show how several oscillatory cycles of short period Q are accommodated in the longer e-folding time P of the exponential expansion. In the lower panel are sketched a few oscillations on an expanded timescale with our present epoch marked. The parameter values have been taken from those given in § 2.3.

of discrete source populations, such as the redshift-magnitude relation, radio source count, angular diameter–redshift relation and the maximum redshifts so far observed, with the choice of the following set of parameters:

$$P \approx 20Q\ , \quad Q \approx 4.4 \times 10^{10}\ \mathrm{yr}\ , \quad \eta = 0.8\ ,$$
$$\Lambda = -0.3 \times 10^{-56}\ \mathrm{cm}^{-2}\ , \quad t_0 = 0.7Q\ .$$

Of these, the last is the present epoch of observation. It is not essential that the model should have only these parameteric values. Indeed, the parameter space is wide enough to make the model robust. Moreover, the fitting of observations to theory does not require postulating ad hoc evolution which is commonly necessary in the case of standard cosmology.

The above framework thus outlines a cosmological model without a beginning and without an end, in which a de Sitter–type exponential expansion, characterized by a very long timescale P, is superposed with finite-size oscillations of a shorter time scale Q. These cycles are statistically identical in their physical properties. In this sense the universe is "quasi-steady." We next see how structures might grow and proliferate in such a universe.

3. A TOY MODEL FOR FORMATION OF STRUCTURES

In an attempt to understand how structures may possibly grow and distribute in space we have carried out the following numerical experiment in two- as well as three-dimensional space. We describe the two-dimensional case first and come to the three-dimensional versions next.

3.1. *Two-dimensional Simulations*

A large number of points ($N \sim 10^5$–10^6), each one representing a mini–creation event, is distributed randomly over a unit square area . The average nearest neighbor distance for such a distribution will then be $(1/\sqrt{N})$. Now suppose that in a typical mini–creation event each particle generates another neighbor particle at random within a distance, $d = x/\sqrt{N}$ in two dimensions. Here the number x is a fraction between 0 and 1 . We shall call x the separation parameter. As explained in § 2.1, the above denotes an ejected piece lying at a distance $\leq d$ from the original compact object.

The sample area is then uniformly stretched by a linear factor $\sqrt{2}$ to represent expansion of space. We now have the same density of points as before, i.e., $2N$ points over area of two units. From this enlarged square remove the periphery so as to retain only the inner unit square.This process thus brings us back to the original state but with a different distribution of an average N points over a unit square. This process is repeated n times . Here the number of iterations, n, plays the role of "time" as in the standard models of structure formation. The number distribution of points evolves as the "creation process" generates new points near the existing ones. We will refer to each point as a "particle" or "unit."

Not surprisingly, soon afterward, i.e., after $n = 3$–4 iterations of the above procedure, clusters and voids begin to emerge in the sample area and create a *Persian carpet* type of patterns. As the experiment is repeated, voids grow in size while clusters become denser. Figure 2 illustrates a typical numerical simulation. It shows that expansion coupled with creation of matter is a natural means of generating voids and clusters. But what of the filaments ?

Here we recall that the creation process near a typical compact massive object will not be isotropic if the mass is spinning. Matter will be preferentially ejected along the axis of spin. To build this effect into the above simulation we adopt the following algorithm.

We assume that in a typical $n > 2$ iteration, the creation of the new neighbor unit C around a typical unit B is not

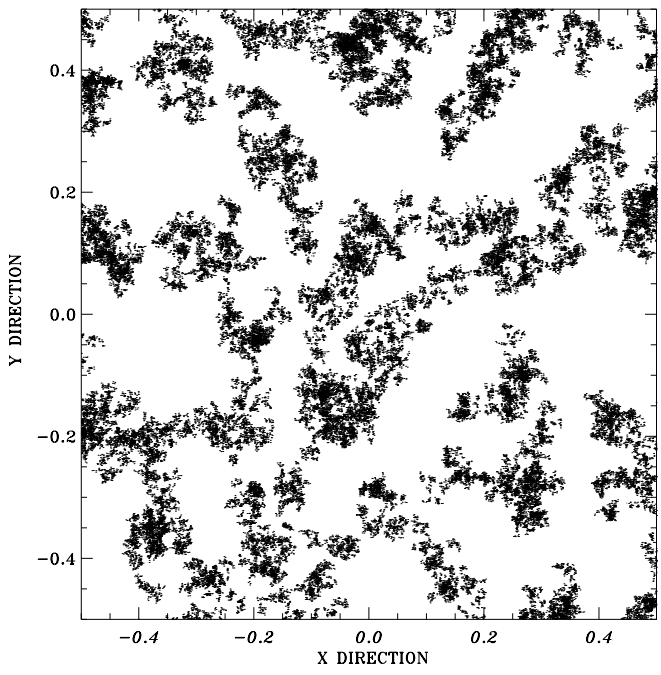

FIG. 2.—A cluster-void distribution generated in the two-dimensional toy model for $N = 100{,}000$ initially randomly distributed particles, with typical separation parameter $x = 0.8$, and the number of iterations $n = 10$. Each particle resembles a galaxy. For further discussion see the text.

entirely random but, instead, is related to the previous history of creation of B from an earlier generation unit A. So the direction BC is broadly aligned with the direction AB in which B itself was ejected. Typically this is ensured by assuming that the ejection is at a random angle in the forward semicircle as explained in Figure 3. We will refer to this as *aligned ejection*, as opposed to the *isotropic ejection* of Figure 2.

Physically this means that the unit B ejected by A retains "memory" of its origin through its spin which is more or less aligned with the spin of A. Which is why when it ejects a unit C, it is more or less aligned with the earlier ejection direction AB.

Although this algorithm does not demand strict alignment, it is interesting to note that the filamentary structure grows along with voids as n increases. Features generated in this way have very suggestive similarities with the observed large-scale structure as shown in a typical simulation of Figure 4. We have also investigated the result of restricting the secondary ejection to a narrower angle, e.g, by keeping the angle φ of Figure 3 in the range $(-\pi/4, \pi/4)$. Not surprisingly we find the filamentary structure more pronounced in such a case. In general, we may argue that the higher the angular momentum per unit mass of the compact object causing ejection, the narrower is the angle of ejection, the greater is the alignment and hence more pronounced the filamentary structure.

Figure 5 shows a typical two-dimensional gravitational clustering simulation data in standard big bang cosmology.

It can be seen that both compact and extended structures are present in both the approaches to structure formation. Since there are no observational data with which comparisons can be made in two dimensions, we shall henceforth deal with the three-dimensional simulations only.

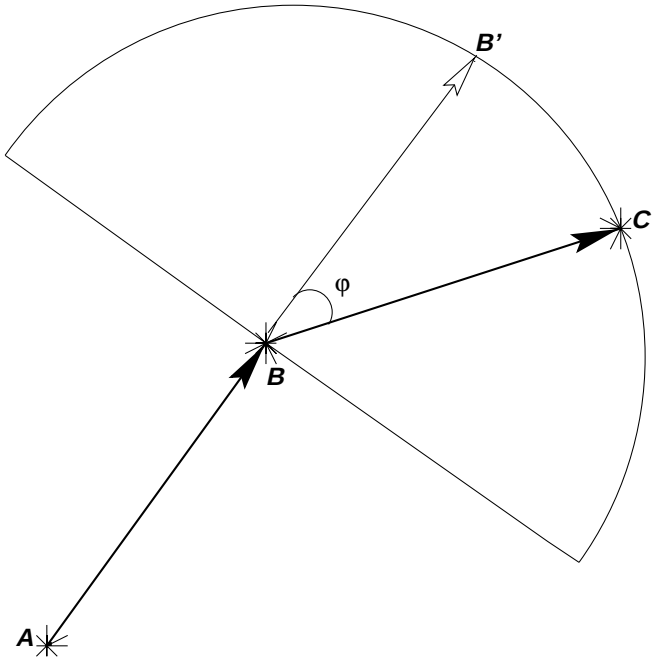

FIG. 3.—Here we schematically show the procedure for creating units in aligned direction for $n > 2$. Point A is a representative of first generation units which are distributed randomly. Point B is a representative of the second generation units, being created in a random direction. Point C represents a third generation unit which has been created in the half-plane lying away from point A off the line perpendicular to AB. BC therefore makes an acute angle, φ, with the line ABB'.

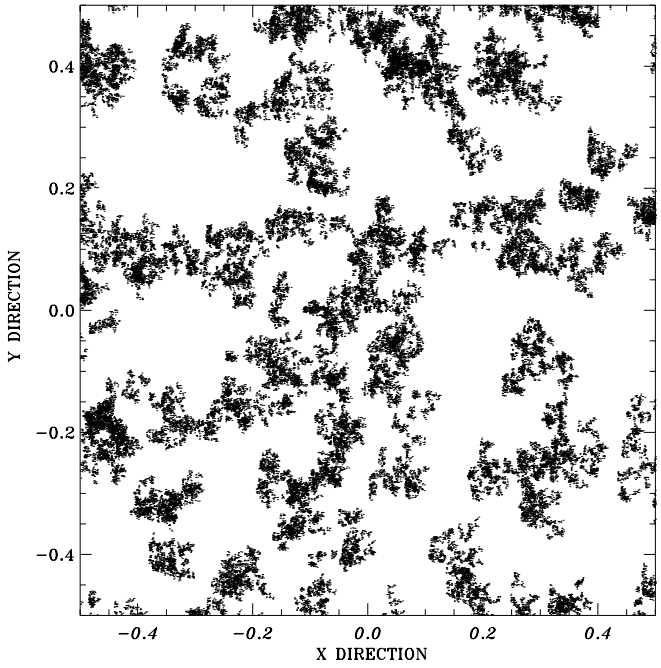

FIG. 4.—A computer-simulated filament-void distribution with $n(>2)$ iterations of aligned ejections having new points following the rule of Fig. 3, for the same parameters of Fig. 2.

3.2. *Three-dimensional Simulations*

The three-dimensional simulation is similar, with the necessary modifications for the higher dimensionality. Thus we start with a unit cube with N points distributed at random within it, the typical interpoint distance being $(1/\sqrt[3]{N})$. Creating a new near neighbor for each particle by

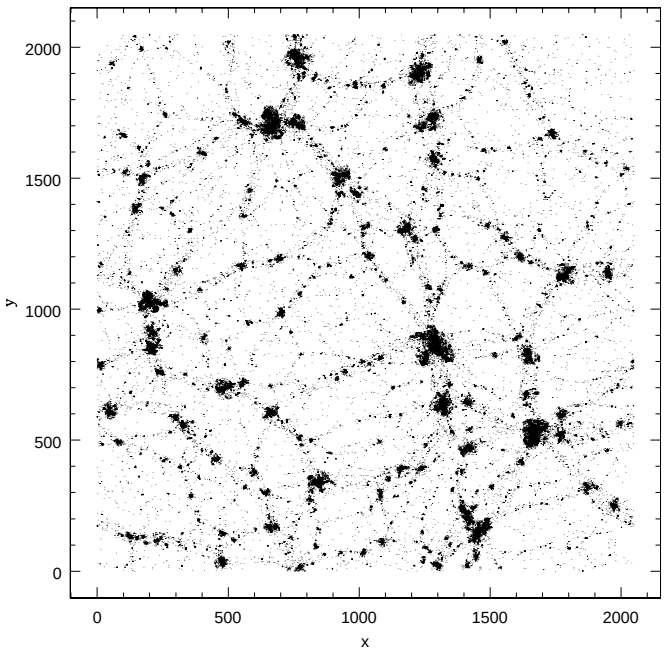

FIG. 5.—A power-law two-dimensional simulation in the standard big bang cosmology for power index, $n = -0.4$ of density fluctuations.

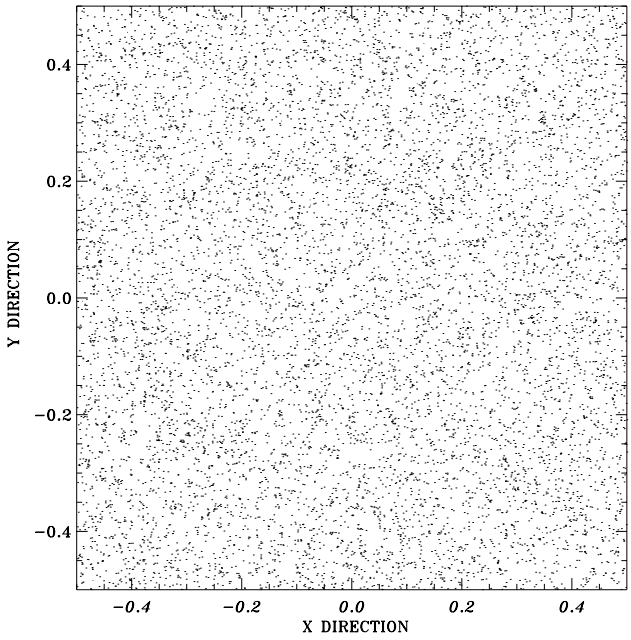

FIG. 6a

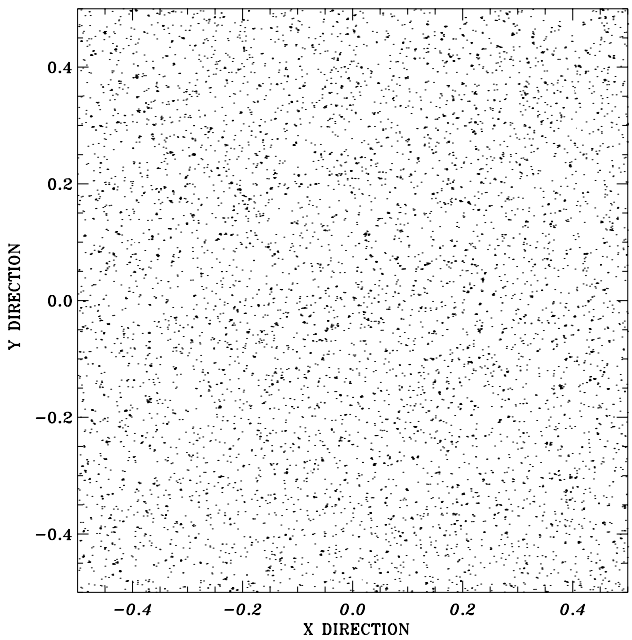

FIG. 6b

FIG. 6.—Three-dimensional version, adapted for the QSSC with $N = 1{,}000{,}000$, $x = 0.3$, $n = 10$, and $P/Q = 20$. Slice thickness in the Z direction is $\Delta Z = 0.01$. Evidently, voids are seen separated by filamentary structures. (*a*) The case of isotropic distribution of particles; (*b*) the case of aligned ejections.

the same rule as in the two-dimensional case, we need to expand each edge of the cube by the factor $\sqrt[3]{2}$. We next apply the same algorithm favoring aligned ejection, suitably modified for three dimensions . To compare the three-dimensional distributions with the observed distributions made up from redshift surveys, we need to take a thin inside slice of the cube perpendicular to one of its edges and examine the distribution of points therein. Before making such a comparison, however, we will first apply three-dimensional simulations within the framework of the QSSC.

3.3. *Simulations of QSSC Cycles*

To bring the toy model closer to the reality of the QSSC, we proceed as follows. We expect the creation activity to be confined largely to a narrow era around a typical oscillatory minimum, when the C-field is at its strongest. By considering the number density of collapsed massive objects at one oscillatory minimum of QSSC to be f, the number density at the next oscillatory minimum would fall to $f \exp(-3Q/P)$ if no new massive objects were added. Thus to restore a steady state from one cycle to the next,

$$\alpha f \equiv [1 - \exp(-3Q/P)]f \sim (3Q/P)f\,, \tag{8}$$

masses must be created anew. In other words, a fraction $3Q/P$ of the total number of massive objects must duplicate themselves in the above fashion.

Notice that, unlike the old steady state theory which had new matter appearing continuously, we have here discrete creation, confined to epochs of minimum of scale factor. The "steady state" is maintained from one cycle to next, which is why the above addition αf is required at the beginning of each cycle.

Therefore, instead of creating a new neighbor particle around each and every one of the original set of N particles, we do so only around αN of these points chosen randomly, where the fraction α is as defined in equation (8). Likewise, the sample volume is homologously expanded by the factor $\exp(3Q/P)$ only instead of by factor 2. We choose the inner cube as before. Figure 6 shows the simulated distributions in cubical slices for isotropic as well as aligned ejections. After a few iterations clusters and voids begin to appear, with the case for aligned ejections showing filaments. For a comparison, see an actually observed distribution of galaxies from a redshift survey in Figure 7.

In the above approximation we have assumed that the creation activity is concentrated at the oscillatory minima. It could be extended over an appreciable part of the oscillatory period, in which case one would see large-scale structure in the radial direction as seen from an observer. We have not modified an algorithm to cover such cases, but we feel that this should be investigated, especially since the recent analysis of the redshift-magnitude relation for supernovae has generated interest in the QSSC models of this kind (Banerjee et al. 1999).

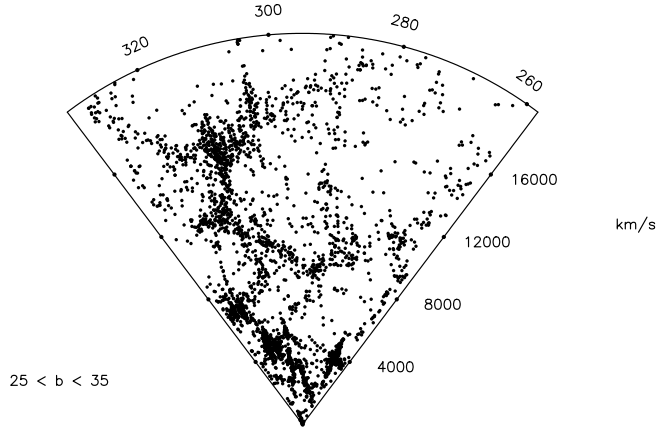

FIG. 7.—A FLAIR redshift survey in the direction of Hydra Centaurus. Data have been taken from Raychaudhury et al. (1995).

4. THE TWO-POINT CORRELATION FUNCTIONS

Although visual inspection of Figures 6 and 7 suggests that the simulation is proceeding along the correct lines, a *quantitative* measure of the cluster-void distribution will help in comparing simulations with reality.

The dimensionless autocorrelation function

$$\xi(r) = \langle[\rho(r) - \langle\rho\rangle][\rho(r_1 + r_1) - \langle\rho\rangle]\rangle/\langle\rho\rangle^2 , \quad (9)$$

where $\langle\rho\rangle$ is the average density in the volume, is one convenient measure of such irregularities in the space distribution. Typically, different classes of objects cluster at different characteristic lengths. To fix ideas in the present model, we will look at distribution of clusters of galaxies. Observationally, it is believed that the two-point correlation function for cluster distribution obeys the following scaling law:

$$\xi_{cc}(r) = \left(\frac{r}{r_0}\right)^{-\gamma} , \quad (10)$$

with $\gamma \simeq 1.8$ and $r_0 = 25\ h^{-1}$ Mpc, where the Hubble constant at the present epoch is taken to be 100 h km s^{-1} Mpc^{-1}. In order to quantify the issues of formation of structures in this scenario we have taken the following measures.

It is known that instead of having a smooth distribution of matter on large scales, the observed universe has structures of typical sizes of a few tens of megaparsecs. These "structures" are regions of density considerably higher than the background density, with the maximum density contrast $\delta = \delta\rho(r)/\langle\rho\rangle$ going from order unity (in the case of clusters) to a few thousand (in the case of the galaxies).

Any process which generates structures must be able to produce to the zeroth order, entities whose density contrast is of such magnitude and with the property that on larger and larger distance scales, the density contrast becomes less significant. This is to ensure that on a large enough scale the universe is homogeneous.

Given this prescription for generating structures without gravitational dynamics, we first ensured that the visual impression created by the cluster simulations did imply that as the number of iterations were increased the number of high-density regions also increased. In the initial configuration one expects to find regions of high density arising only because of the Poisson noise. In the later "epochs" after a few iterations, however, we expected and did find that the variation of the one-point distribution function for density $\rho/\langle\rho\rangle$, with $\langle\rho\rangle$ the average density in the volume, showed a steady and significant increase in the the number of high- and intermediate-density regions, as is expected in a clustering scenario. We further observed that the value of maximum density also increased as a function of the number of iterations, which in this experiment corresponds to "time." The density field has been generated on a grid placed into the simulation volume using the algorithm of cloud in cell.

Our simulations show the growth of structures through rise in the density maximum as a function of number of iterations. The aligned ejection mode leads to faster clustering than the isotropic one. One must also examine the dependence of this "growth" on another important parameter in this prescription, namely the typical maximum separation between a creation site and the unit which is created. This was indicated by the parameter x in our earlier discussion.

Again our studies investigate results of the structure formation algorithm when the parameter x is changed. We find that higher densities are achieved when this distance (in units of box size) is made smaller. This is intuitively expected. In the QSSC case, clustering is stronger in the early epochs for the isotropic ejection model, although at a later stage the density function for the aligned ejection model catches up and ultimately exceeds the rate for the isotropic case.

The next quantitative measure that we computed from this data set was the two-point correlation function. The following figures summarize the results of these computations. It can be seen that the observationally obtained power-law dependence of the two-point correlation function $\xi(r) = (r_0/r)^{1.8}$ can be obtained, provided that a sufficient number of iterations has been performed, i.e., a sufficient length of "time" has elapsed.

Figure 8 shows the two-point correlation function for the case of the QSSC-based model. As "time" goes on, the slope of the correlation function gets closer and closer to -1.8. From the value of the X-axis intercept of the two-point correlation function it is possible to get a rough estimate of the size of the structures in units of the size of our simulation box. From our results we have estimated that the size of the structures formed is approximately $\beta = 0.15$–0.3 times the box size. If one sets these values equal to the observationally accepted value of r_0, one can get a better physical sense of the results. If we set, $\beta = 0.3$, say, and $r_0 = 25\ h^{-1}$ Mpc, then the linear size of the simulation box would be $\sim 84\ h^{-1}$ Mpc.

The above exercise is an attempt to relate our toy model to a realistic cosmological scenario. The model per se talks of a "dimensionless" box containing N points. With the above identification, we have 10^5 points in a volume of $(84h^{-1})^3$ Mpc^3. Let us assign a mass of $10^n\ M_\odot$ to each

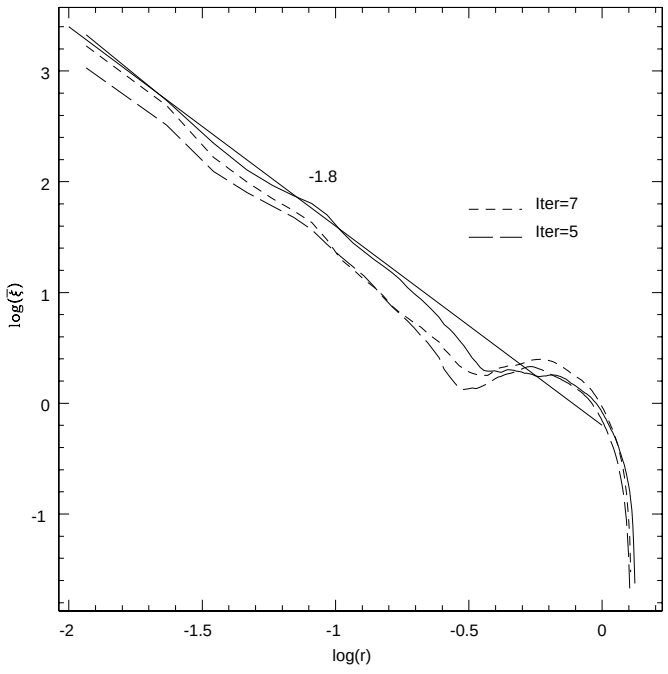

FIG. 8.—The two-point correlation function for the QSSC based model. $N = 100{,}000$ and $x = 0.3$. As "time" goes on, the curve approaches more and more closely the slope of -1.8. The solid curve shows the result after 10 iterations.

point. We then get a cosmological smoothed out density of

$$\rho = \frac{10^{n+5}\ M_{\odot}}{(84\ h^{-1})^3\ \mathrm{Mpc}^3} = 0.6\ h \times 10^{n-12}\rho_c\ , \qquad (11)$$

where ρ_c is the critical density of the universe. Thus we get the density parameter $\Omega = 0.6\ h \times 10^{n-12}$. Setting this equal to unity (the QSSC does not have any limit on baryonic matter either from deuterium abundance or from CMBR anisotropy), we get for $h = 0.6$, a typical mass as $1.5 \times 10^{13} M_{\odot}$, suitable for a cluster.

Of course, as the above exercise shows, the results can be scaled up/down by rescaling the simulation parameters and thus are independent of the "absolute" size of the box. A more detailed dynamical theory of the creation process will tell us how to relate the absolute size of clustering to the theoretical parameters.

5. CONCLUSION

It must be stressed that these results are to be viewed as a preliminary report on a new scheme for generating structures in the quasi–steady state cosmology and quite a lot of follow-up work has to be put into refining the model so as to arrive at the values of the various parameters (chosen so far in an empirical way) from a deeper theoretical standpoint. Whatever the details of the creation process, the QSSC has repeated oscillations. We are trying to understand, with the help of probability theory and stochastic processes, how clustering develops through such an iterative program. An analytical result, if it exists, will be far more illuminating than repeated simulations.

The primary statistical indicator we have used in our analysis is the two-point correlation function $\bar{\xi}(r)$. In order to further examine the statistical properties of the particle distribution, one must investigate the behavior of higher moments and other quantities such as the "shape statistics." Work analyzing the higher moments, scaling relations, shape statistics, and so on using algorithms such as counts in cells is in progress. We plan to address all these issues in detail in a future work.

However, the problem of formation of large-scale structure being a complex one, it is desirable to keep the theoretical options open in the underlying cosmology. At the risk of stating the obvious, we should contrast the present approach from the standard approach to structure formation in the big bang cosmology. In the standard approach primordial fluctuations are postulated to begin with and their growth is studied under the effect of the gravitational field. Here the main process which generates structures in the universe is the creation of matter around MCEs rather than gravitational instability. Our computer simulations show very clearly that the filament-cluster-void pattern observed in large-scale structure can be generated simply from a creation algorithm. To what extent gravitational effects will further influence this picture remains to be seen. More sophisticated simulations together with gravitational instability would be needed to follow up this work. Although we have given preliminary ideas in § 2.1, a more detailed cosmogonic theory is also needed to tell us how coherent objects are ejected by mini–creation events. The success of the present toy model, however, holds out hope for a better understanding of structure formation via this alternative route.

We thank the referee of this paper for making several constructive comments that have led to an improved version. J. V. N. thanks the Department of Atomic Energy for a Homi Bhabha Research Professorship. A. N. acknowledges a research fellowship from the University Grants Commission, while S. E. acknowledges a senior research fellowship from the Council of Scientific and Industrial Research. All three thank IUCAA for its computational and other facilities.

REFERENCES

Banerjee, S. K., & Narlikar, J. V. 1997, ApJ, 487, 69
Banerjee, S. K., Narlikar, J. V., Hoyle, F., Burbidge, G., & Sandage, A. 1999, preprint
Hoyle, F., Burbidge, G., & Narlikar, J. V. 1993, ApJ, 410, 437
———. 1994a, MNRAS, 267, 1007
———. 1994b, A&A, 289, 729
———. 1995a, Proc. R. Soc. London A, 448, 191
———. 1995b, MNRAS, 277, L1
Hoyle, F., & Narlikar, J. V. 1964, Proc. R. Soc. London A, 282, 191
———. 1966, Proc. R. Soc. London A, 294, 138
Padmanabhan, T. 1993, Structure Formation in the Universe (Cambridge: Cambridge University Press)
Peebles, P. J. E. 1993, Principle of Physical Cosmology (Princeton: Princeton University Press)
Raychaudhury, S., Colless, M., & Hola, R., 1994, in Proc. 35th Herstmonceux Conf. Wide-Field Spectroscopy and the Distant Universe, ed. S. J. Maddox & A. Aragon-Salamanca (Singapore: World Scientific), 110–114
Sachs, R., Narlikar, J. V., & Hoyle, F. 1996, A&A, 313, 703